Low-temperature synthesis of strain sensor based on flexible ZnO nanowire-cellulose paper composite

Indranil Biswas, Piyali Roy (Kundu), Mousumi Majumder, Suman Sau, Ashim Kumar Chakraborty ✉

Materials Characterization and Instrumentation Division, CSIR-Central Glass & Ceramic Research Institute, Jadavpur, Kolkata 700032, India
✉ *E-mail: ashim3121@gmail.com*

Published in Micro & Nano Letters; Received on 23rd February 2017; Accepted on 9th March 2017

ZnO nanowire was synthesised chemically at low temperature on a flexible three-dimensional and porous cellulose paper. The morphology and crystallography of the composite was characterised by field emission scanning electron microscope and X-ray diffraction. Performance of the developed ZnO nanowire-cellulose paper composite as strain sensor demonstrated good stability, high gauge factor and good repeatability. The results indicate the possible use of this sensitive and robust strain sensor in the fields of biomedical sciences, MEMS devices and structural health monitoring and other fields.

1. Introduction: Crystalline ZnO-based piezoelectric sensors are gaining attention from researchers in recent times due to their ability to convert mechanical energy into electrical energy and requirement of lower input power. To measure strain, a crystalline piezoelectric material is generally bonded to the surface of the host structure or embedded in it. However, such materials are generally brittle and weak under tension and hence cannot be used in places where flexibility is a criterion. Besides, simultaneous application of mechanical and electrical load can damage such materials. Thus a simple, scalable, low cost and flexible piezo-composite sensor is required for effective strain sensing. Zinc oxide is a biocompatible semiconductor with a wide bandgap of 3.37 eV at room temperature [1] and has useful properties like piezoelectric properties (piezoelectric co-efficient = 12 pC/N) and high electron mobility at room temperature ($\mu_e = 200$ cm^2/V s) [2]. It is abundantly available in nature and has a wide range of applications such as in strain sensing [3], acoustic sensing [4], energy harvesting [5] etc. In this Letter, we report low-temperature synthesis of a composite material consisting of ZnO and cellulose paper (ZnOCP) and its strain sensing application under static loading. The cellulose paper matrix helps to make the composite structure flexible. Under static tensile loading, its performance is comparable with that of a commercially available strain sensor.

2. Experimental

2.1. Chemicals/materials: Zinc acetate (Merck), ethanol (Merck), sodium hydroxide (Merck) and cellulose paper ($\phi = 9$ cm, thickness = 0.06 mm).

2.2. Synthesis process: ZnOCP composite material was synthesised following the steps outlined in Fig. 1 [6]. To prepare ZnOCP composite, non-aqueous solutions of zinc acetate (0.1 M) and sodium hydroxide (1 M) were prepared by dissolving each in 50 ml ethanol at 60°C. A cellulose paper ($\phi = 9$ cm and thickness = 0.06 mm) was placed in a glass petri dish and the paper was soaked in zinc acetate (0.1 M) solution for 5 h at 60°C. The soaked paper was air-dried, followed by drying at 100°C for 1 h in a closed furnace. The paper was then dipped into sodium hydroxide (1 M) for 5 h at a temperature 60°C and dried at 100°C for 1 h. Due to hydrolysis, ZnO nanoparticles were formed on the surface of the cellulose fibres. The ZnO-coated cellulose paper was then washed with distilled water and dried in a closed furnace at 100°C for 1 h to remove the by-products.

$$\begin{aligned} &Zn(CH_3COO)_2 + NaOH \rightarrow CH3COONa + Zn(OH)_2 \\ &Zn(OH)_2 \rightarrow ZnO + H_2O \end{aligned} \quad (1)$$

2.3. Characterisation: X-ray diffraction was performed on the ZnOCP composite for phase identification using Bruker D8 Advance Davinci XRD system with Cu Kα radiation ($\lambda = 1.54$ Å, 1.6 kW, 40 mA). Surface morphology of the sample was determined using ZEISS (SIGMA) field emission scanning electron microscope (FESEM).

2.4. Strain characterisation: The ZnOCP composite (3.0 cm × 1.0 cm) was mounted on a dog bone-like structure made of phosphor bronze ($E = 120$ GPa, thickness = 0.4 mm) as shown in Figs. 2 and 4*a*.

Phosphor bronze, being an elastic material can efficiently transfer strain to the ZnOCP composite. The ZnOCP composite was mounted on the dog bone structure using adhesive (CYANOACRYLATE, Tokyo Sokki Ken Kyuio Co. Ltd. Japan). The adhesive enables effective transfer of strain from the phosphor bronze substrate to the ZnOCP sensor affixed on its surface. Two electrodes were made (1 cm apart) on the surface of the mounted film using silver conductive adhesive (Alfa aesar). Induced charge and *I–V* measurements were done using a source and measuring unit (Make: Keithley, Model: 6517). Initially, the ZnOCP composite was poled by applying a 20 V DC voltage for 1 min and then shorting the terminals for 1 min to drain out the residual charges [6]. A potential difference was applied between the electrodes of the ZnOCP composite and the corresponding current was measured. The potential sweep was set at a constant rate of 0.02 V/s and was varied from 0 to 5 V. Simultaneous strain measurement was done in the tensile mode using pull test equipment (Instron) as shown in Figs. 3 and 4*c*. Stress is measured with the help of load cells attached to the equipment. The ZnOCP composite attached to the phosphor bronze structure was fixed between the grips of the equipment and the strain was precisely controlled.

In this study, stretching speed was set to 1.5 µm/s. A foil strain gauge (Tokyo Sokki Ken Kyuio Co. Ltd. Japan, gauge resistance: 120 Ω, gauge factor: 2.05) was attached along the length of the phosphor bronze structure for comparison of the strain values. After applying strain along the length of the dog bone structure, corresponding *I–V* data were recorded. Measurement of induced charge developed due to piezoelectric effect was also done using the pico-ammeter (Make: Keithley, Model: 6517) at

doi: 10.1049/mnl.2017.0114

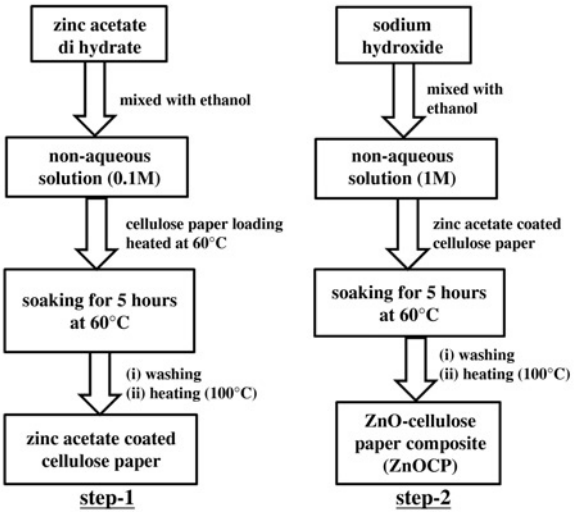

Fig. 1 *Schematic of synthesis process of ZnOCP composite*

different strain values under zero bias potential applied between the electrodes.

3. Result and discussion

3.1. Structure and morphology: Fig. 5 shows the XRD patterns of cellulose paper and ZnOCP. A low-intensity broad peak of cellulose is seen at $2\theta = 21.3°$ and high-intensity narrow peaks at $2\theta = 32.01°$, 34.69°, 36.50°, 47.76°, 56.85°, 63.07° and 68.14° corresponding to the polycrystalline wurtzite structure of ZnO. The strongest peak of ZnO is found along the (101) plane.

No peaks corresponding to metal hydroxides were seen in the XRD pattern of ZnOCP. Average crystallite size (D) of ZnO nano particles was calculated to 20–30 nm using Scherrer's (2) [7]

$$D = \frac{K\lambda}{\beta \cos\theta} \tag{2}$$

where $K = 0.94$ is the Scherrer's constant, $\lambda = 1.5406$ Å, 2θ is the Bragg's diffraction angle and β is the full width at half maximum intensity of the ZnO peaks.

Figs. 6*a* and *b* show FESEM micrographs of the cellulose paper and ZnOCP composite, respectively. The primary cellulose paper (Fig. 6*a*) is porous and composed of micrometre sized randomly oriented smooth cellulose fibres.

Fibbers become very rough after ZnO coating on it, as seen in Fig. 6*b*. The high-magnification micrograph (Fig. 6*c*) shows dense, uniform distribution of ZnO nano particles throughout the cellulose matrix. The material is hence expected to possess uniform piezoelectric behaviour.

3.2. Strain sensing and measurement of induced charge: Piezoelectric charge density was measured using a pico-ammeter (Make: Keithley, Model: 6517) under different strain conditions following the relation (3):

$$\text{Piezoelectric charge density} = Q/A \tag{3}$$

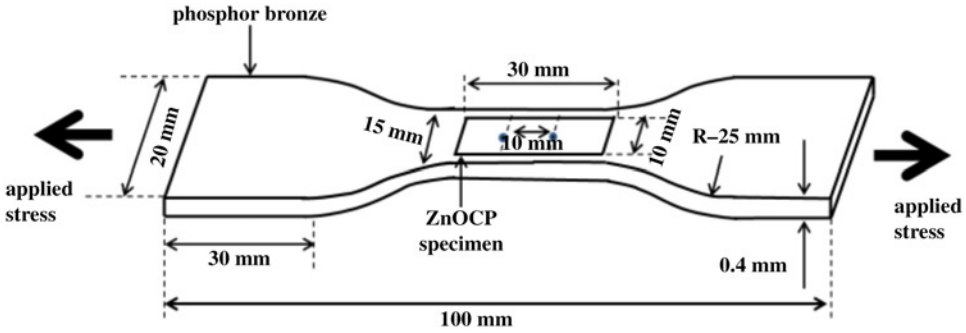

Fig. 2 *Schematic of dog bone-like structure made of phosphor bronze used in the strain measurement*

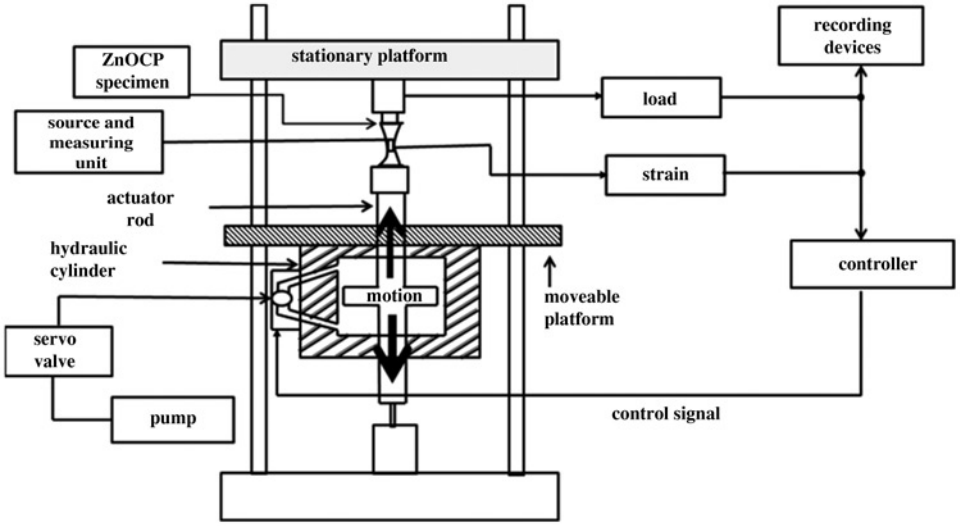

Fig. 3 *Schematic of the tensile mode strain measurement setup*

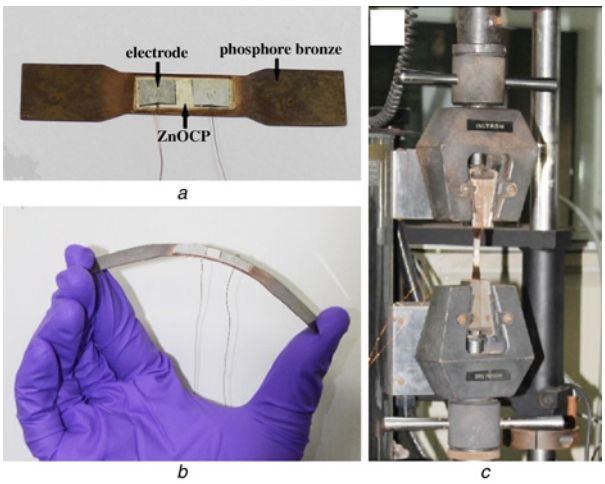

Fig. 4 *Optical image of the fabricated device and measurement set up*
a Optical image of the final device
b Optical image showing the flexibility of the developed sensor mounted on a dog bone-like structure made of phosphor bronze
c Optical image of the tensile mode strain measurement setup (Instron)

where Q is the induced piezoelectric charge and A is the electrode area.

Fig. 7 shows that the induced charge generated due to piezoelectric effect, increases with the increase in tensile strain [8]. It was observed that flexibility of the cellulose paper was fairly retained after ZnO coating. Ion displacement occurs when the ZnO fibre is strained on elongation, this in turn, develops positive charge on the ZnO/Ag interface and generates a piezoelectric potential between the electrodes. This potential increases the Schottky barrier height as

$$\Delta\phi_{\mathrm{B}} = q\rho_{\mathrm{p}}w_{\mathrm{p}}^2/2\varepsilon_{\mathrm{s}} \tag{4}$$

where $\Delta\phi_{\mathrm{B}}$ is the change in Schottky barrier, w_{p} is the width of the polarisation layer on the interface, ε_s is the permittivity of the piezo material, ρ_{p} is the density of polarisation charges, and q is the value of unit electronic charge. The change in Schottky barrier height

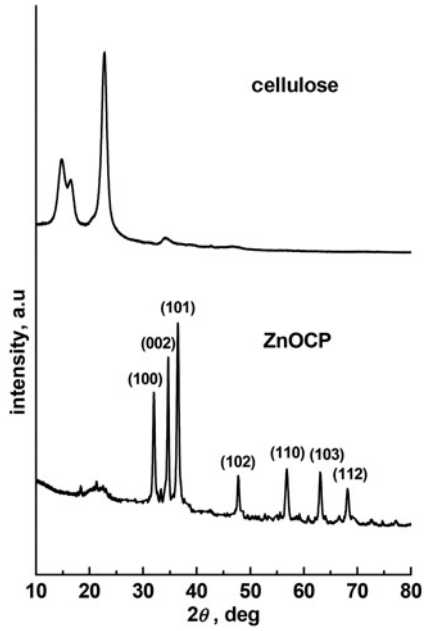

Fig. 5 *XRD patterns of the cellulose and ZnOCP*

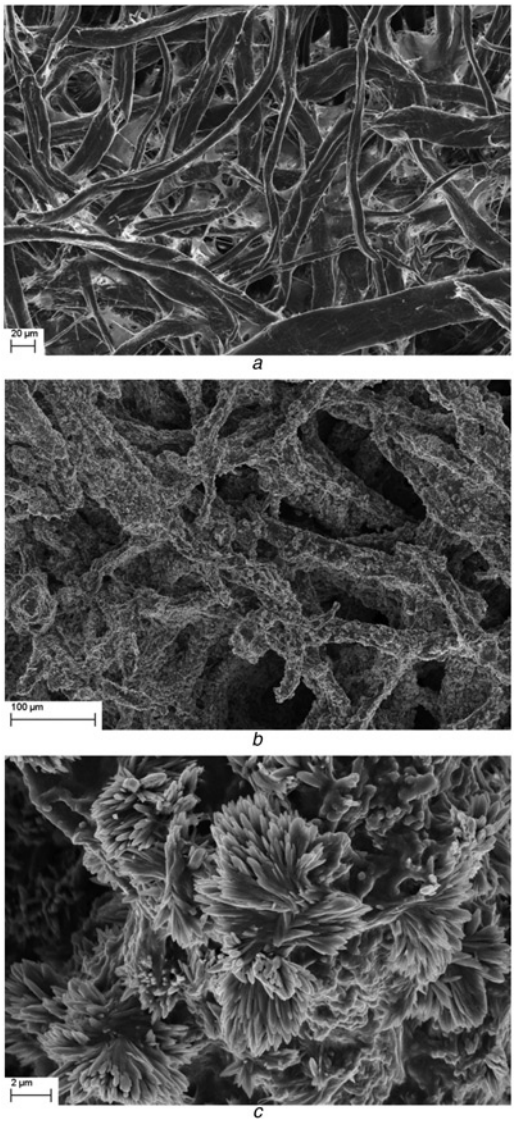

Fig. 6 *FESEM micrograph*
a FESEM micrograph of cellulose paper
b FESEM micrograph of ZnOCP
c High-magnification FESEM micrograph of ZnOCP

$\Delta\phi_{\mathrm{B}}$ is thus proportional to the applied strain as $\rho_{\mathrm{p}} \propto$ applied strain. Any change in the applied strain will therefore result in a shift of the I–V curves of the nano composite. From the I–V

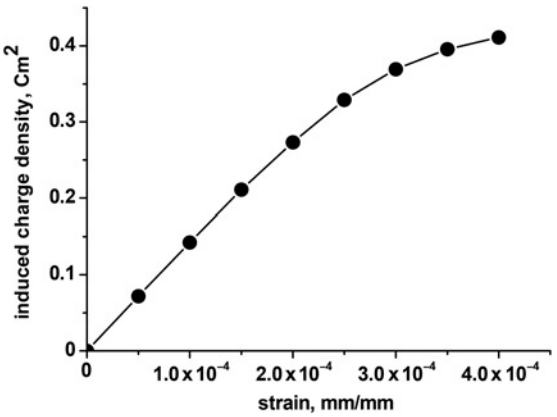

Fig. 7 *Strain-charge density curve of ZnOCP*

doi: 10.1049/mnl.2017.0114

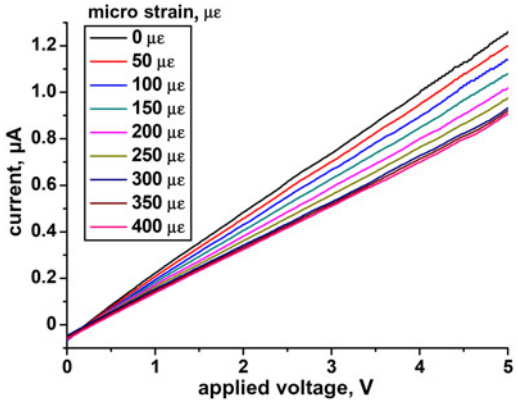

Fig. 8 *I–V characteristics of the ZnOCP composite as a function of strain*

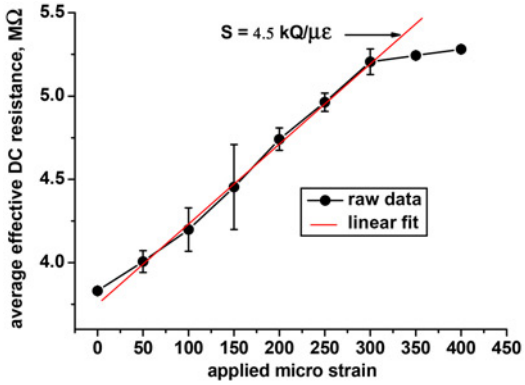

Fig. 9 *Average effective DC resistance of ZnOCP for different strain values is computed, and their corresponding error bars (i.e. using the standard deviation) are also shown*

curve shown in Fig. 8, it is clear that a Schottky barrier is present at the ZnO/Ag interface which plays an important role in the electrical transport of ions in the ZnOCP composites [9–11].

Fig. 8 shows that the *I–V* curves are fairly linear. Good repeatability of the measurements was observed when the applied strain was slowly withdrawn. Effective DC resistance was measured from the slope of the *I–V* curve and found to be increasing with the increase in strain (Fig. 8). A series of similar *I–V* measurements were conducted at different strain values for obtaining a good statistical representation of sensor performance.

The sensors average sensitivity (S) is equivalent to the slope of the least-squares fitted line (Fig. 9) and can be calculated as

$$S = \Delta R/\Delta\varepsilon \tag{5}$$

where ΔR is the change in resistance and $\Delta\varepsilon$ is the change in applied microstrain.

In this study, the average sensitivity achieved is 4.5 kΩ/με.

For all practical applications, the performance of a strain sensor is characterised by its gauge factor defined by (6)

$$\mathrm{GF} = \left(\Delta R/R_0\right)/\varepsilon \tag{6}$$

where ΔR is the change in resistance and R_0 is the initial resistance ($\varepsilon = 0$).

From the slope of the least-squares fitted line (Fig. 10), measured average gauge factor of the reported ZnOCP composite strain sensor was found to be 1183, which is higher than the gauge

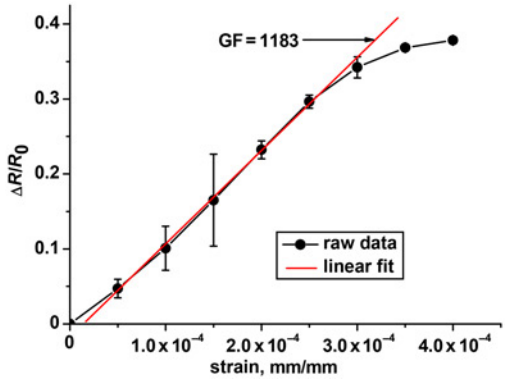

Fig. 10 *Resistance variation–strain relationship of ZnOCP under static tensile loading and their corresponding error bars (i.e. using the standard deviation) are also shown*

factors of conventional metallic strain gauges (~1 to 5), Si strain sensors (~200), as well as CNT (~1000)-based devices [12].

4. Conclusion: Synthesis and characterisation of a composite strain sensor based on ZnO-cellulose paper is reported in this study. The sensor was fabricated by a low-temperature chemical route. *I–V* characterisation of the device shows linear response at different strain values. The sensor device has good stability and high gauge factor (~1183) which indicates its possible use in the fields of biomedical sciences, MEMS devices, structural health monitoring etc.

5. Acknowledgments: This work has been carried out under the project ESC 0103 funded by CSIR. The authors express their gratitude to Director, CSIR-CG&CRI for support in carrying out the research work. The cooperation from AMMCD, CSIR-CGCRI during this research work is also acknowledged.

6 References

[1] Oprea O., Aderonescu E., Ficai D., *ET AL.*: 'ZnO applications and challenges', *Curr. Org. Chem.*, 2014, **18**, pp. 192–203

[2] Gao P.X., Wang Z.L.: 'Nanoarchitectures of semiconducting and piezoelectric zinc oxide', *J. Appl. Phys.*, 2005, **97**, pp. 0443041–0443047

[3] Zhou J., Fei P., Gu Y., *ET AL.*: 'Pezoelectric-potential-controlled polarity-reversible Schottky diodes and switches of ZnO wires', *Nano Lett.*., 2008, **8**, pp. 3973–3977

[4] Du X.Y., Fu Y.Q., Tan S.C., *ET AL.*: 'ZnO film for application in surface acoustic wave device', *J. Phys. Conf. Ser.*, 2007, **76**, pp. 012035 doi: 10.1088/1742-6596/76/1/012035

[5] Wang Z.L., Song J.: 'Piezoelectric nanogenerators based on zinc oxide nanowire arrays', *Science*, 2006, **312**, pp. 242–246

[6] Gullapalli H., Vemuru V.S.M., Kumar A., *ET AL.*: 'Flexible piezoelectric ZnO-paper nanocomposite strain sensor', *Small*, 2010, **6**, pp. 1641–1646

[7] Azaroff L.V.: 'Elements of X-ray crystallography' (McGraw Hill Book Co, New York, 1968)

[8] Ko H.U., Mun S., Min S.K., *ET AL.*: 'Fabrication of cellulose ZnO hybrid nanocomposite and its strain sensing behavior', *Materials*, 2014, **7**, pp. 7000–7009

[9] Zhang W., Zhu R., Nguyen V., *ET AL.*: 'Highly sensitive and flexible strain sensors based on vertical zinc oxide nanowire arrays', *Sens. and Act. A Phys.*, 2013, **205**, pp. 164–169

[10] Zhou J., Gu Y., Fei P., *ET AL.*: 'Flexible piezotronic strain sensor', *Nano Lett.*., 2008, **8**, (9), pp. 3035–3040

[11] Zhang Y., Liu Y., Wang Z.L.: 'Fundamental theory of piezotronics', *Adv. Mater.*, 2011, **23**, pp. 3004–3013

[12] Cao J., Wang Q., Dai H.J.: 'Electromechanical properties of metallic, quasimetallic, and semiconducting carbon nanotubes under stretching', *Phys. Rev. Lett.*, 2003, **90**, pp. 157601.1–157601.4